11.2 A REAL-TIME MODIS VEGETATION COMPOSITE FOR LAND SURFACE MODELS AND SHORT-TERM FORECASTING

Jonathan L. Case[1]*, Frank J. LaFontaine[2], Sujay V. Kumar[3], and Gary J. Jedlovec[4]

[1]ENSCO, Inc./Short-term Prediction Research and Transition (SPoRT) Center, Huntsville, AL
[2]Raytheon/SPoRT Center, Huntsville, AL
[3]SAIC/NASA Goddard Space Flight Center, Greenbelt, MD
[4]NASA Marshall Space Flight Center/SPoRT Center, Huntsville, AL

1. INTRODUCTION

An important variable that especially impacts the transport of moisture into the atmosphere during the warm season is evapotranspiration from vegetative surfaces. Vegetation is represented in models by the horizontal and vertical distribution of plant vegetation given by the Greenness Vegetation Fraction (GVF) and Leaf Area Index (LAI), respectively (Gutman and Ignatov 1998). The operational Noah land surface model (LSM; Chen and Dudhia 2001; Ek et al. 2003) as found in the Weather Research and Forecasting (WRF) model (Skamarock et al. 2008) and National Centers for Environmental Prediction (NCEP) North American Mesoscale model (Janjic et al. 2001; Janjic 2003) holds the LAI fixed for all vegetation classes.

The GVF, meanwhile, is allowed to vary spatially in the Noah LSM according to a global monthly climatology dataset derived from Normalized Difference Vegetation Index (NDVI) data on the NOAA Advanced Very High Resolution Radiometer (AVHRR) polar orbiting satellite, using information from 1985 to 1991 (Gutman and Ignatov 1998; Jiang et al. 2010). Representing data at the mid-point of every month (e.g. June climatology is valid for the 15th of the month), this monthly climatological dataset is on a grid with 0.144° (~16 km) spatial resolution and has been implemented into the operational Noah LSM at NCEP and within the community WRF model (Ek et al. 2003; Jiang et al. 2010; Skamarock et al. 2008).

A limitation that the climatological dataset presents is that the annual cycle of GVF is always represented the same in models from one year to the next. In reality, the response of vegetation to meteorological and climate conditions varies between seasons and years based on anomalous weather and climate features. Extreme events such as an unusual hard freeze, late bloom due to colder than average temperatures, or drought can lead to a vegetative response that is quite different than the climatological representation. In addition, the dated nature of the GVF climatology and relatively coarse resolution may not be representative of current vegetative conditions in today's high-resolution numerical models. Recent land use changes due to urbanization since the period of record of the GVF climatology likely contribute to mis-representations in the models.

*Corresponding author address: Jonathan Case, ENSCO, Inc., 320 Sparkman Dr., Room 3062, Huntsville, AL, 35805. Email: Jonathan.Case-1@nasa.gov

Therefore, the NASA Short-term Prediction Research and Transition (SPoRT) Center proposes a Continental U.S. (CONUS) scale, high resolution GVF dataset that is updated on a daily basis with near real-time swath data from the Moderate Resolution Imaging Spectroradiometer (MODIS) instruments aboard the NASA Earth Observing System Aqua and Terra satellites. This new dataset is inserted into the NASA Land Information System (LIS) to improve the representation of land surface processes within the Noah LSM in LIS, and ultimately in the WRF model via the coupling to LIS. The GVFs are derived from NDVI data that are produced in near real-time from the Aqua and Terra platforms. The NDVI is based on properties of healthy vegetation, which has a high absorbance (low reflectance) in the visible portion (or photosynthetically active region) of the electromagnetic spectrum while having a high reflectance at the near-IR wavelengths. Thus, the NDVI is defined as the combination of these reflectances:

$$NDVI = \frac{\rho_{NIR} - \rho_{RED}}{\rho_{NIR} + \rho_{RED}} \qquad (1),$$

where ρ_{NIR} is the satellite reflectance at near-IR wavelengths (0.75–1.5 μm) while ρ_{RED} is the satellite reflectance at visible-red wavelengths (0.6–0.7 μm). NDVI ranges from -1 to +1, where a value near +1 indicates a healthy, fully-vegetated surface. Values near 0 indicate little to no vegetation while negative values typically correspond to snow or ice cover under clear sky conditions.

Experiments with real-data and/or near real-time vegetation in place of the operational climatological dataset are not new. Previous studies have examined near real-time vegetation datasets derived from the NOAA/AVHRR satellite (Jiang et al. 2010) and its potential utility on real-time modeling (Crawford et al. 2001; Kurkowski et al. 2003; James et al. 2009). Few studies, however, have examined such datasets derived from the NASA MODIS instruments (Miller et al. 2006; Ruhge and Barlage 2011), particularly with real-time MODIS data at high spatial resolution (1-km) for regional, real-time high-resolution modeling applications (e.g. Kain et al. 2010). This paper and companion presentation describes the development of a CONUS-scale, 1-km real-time MODIS NDVI/GVF product to replace the coarser-resolution climatological GVFs currently implemented in the NASA LIS and operational models. Section 2 gives some background information on the NASA SPoRT Center. Section 3 provides a brief overview of the NASA LIS land surface modeling framework. Section 4 describes

the real-time production of the SPoRT NDVI composites and how the GVF is computed for use within LIS. Preliminary results from offline LIS-Noah runs are presented in Section 5 followed by a summary and future direction presented in Section 6.

2. NASA SPORT CENTER

The NASA SPoRT Center at the Marshall Space Flight Center (MSFC) seeks to accelerate the infusion of NASA Earth Science observations, data assimilation, and modeling research into weather forecast operations and decision-making at the regional and local level (Goodman et al. 2004). It directly supports the NASA strategic plan of using results of scientific discovery to directly benefit society. The program is executed in concert with other government, university, and private sector partners. The primary focus is on the regional scale and emphasizes forecast improvements on a time scale of 0–24 hours. The SPoRT Center has partnered with and facilitated the use of real-time NASA data and products to 17 National Weather Service (NWS) Weather Forecast Offices (WFOs) primarily in the Southern Region, as well as several private weather entities. Numerous new techniques have been developed to transform satellite and lightning observations (Darden et al. 2010) into useful parameters that better describe changing weather conditions, including proxy products that demonstrate utility for the upcoming GOES-R satellite era (Stano et al. 2010).

The unique weather products have helped local WFOs improve forecasts of reduced visibility due to fog, low clouds, and smoke and haze from sources such as forest fires and agricultural burning, the onset of precipitation, the occurrence and location of severe weather events, and assess other local weather changes. Additionally, high-resolution satellite data provided by SPoRT has been used by the private sector to inform the marine weather community of changing ocean conditions and with tropical storm and hurricane monitoring.

3. LAND INFORMATION SYSTEM DESCRIPTION

The NASA LIS is a high performance land surface modeling and data assimilation system that integrates satellite-derived datasets, ground-based observations and model reanalyses to force a variety of LSMs (Kumar et al. 2006). By using scalable, high-performance computing and data management technologies, LIS can run LSMs offline globally with a grid spacing as fine as 1 km to characterize land surface states and fluxes.

Case et al. (2008) presented improvements to simulated sea breezes and surface verification statistics over Florida by initializing the WRF model with land surface variables from an offline LIS spin-up run, conducted on the same WRF domain and resolution. In addition, Case et al. (2011) demonstrated the utility of using both the LIS land surface fields and high-resolution MODIS SSTs (Haines et al. 2007) to initialize the surface variables over the southeastern U.S., thereby providing a high-resolution lower boundary initial condition over the entire modeling domain that contributed to slight improvements in modeled summertime precipitation systems.

To compare the SPoRT GVFs to the climatology GVFs, the LIS is configured to use the International Geosphere-Biosphere Programme (IGBP) land-use classification (Loveland et al. 2000) as applied to the MODIS instrument (Friedl et al. 2010). All static and dynamic land surface fields are masked based on the IGBP/MODIS land-use classes. The soil properties are represented by the State Soil Geographic (STATSGO; Miller and White 1998) database. Additional required parameters include quarterly climatologies of albedo (Briegleb et al. 1986), a 0.05° resolution maximum snow surface albedo derived from MODIS (Barlage et al. 2005), monthly climatologies of greenness fraction data derived from AVHRR in the control LIS simulations (Gutman and Ignatov 1998), and a deep soil temperature climatology (serving as a lower boundary condition for the soil layers) at 3 meters below ground, derived from 6 years of Global Data Analysis System (GDAS) 3-hourly averaged 2-m air temperatures using the method described in Chen and Dudhia (2001).

4. EXPERIMENTAL NDVI/GVF DATASET

4.1 MODIS NDVI Compositing algorithm

The NASA SPoRT Center has been producing daily real-time, 0.01 degree (~1-km) resolution MODIS NDVI gridded composites over a Continental U.S. (CONUS) domain since 1 June 2010. The geographical extent of the CONUS grid ranges from 23°N to 52°N latitude and 128°W to 65°W longitude. These composites are updated daily based on swath data from the MODIS sensor aboard the polar orbiting NASA Aqua and Terra satellites, with a product time lag of about one day.

Figure 1 illustrates the data flow and processing that occurs during the course of creating a single day's NDVI composite. NDVI swath and cloud mask data are received from the University of Wisconsin, and each swath is individually mapped onto the CONUS 1-km grid using McIDAS utilities (left column of Figure 1). A simple time-weighting algorithm is applied to the remapped NDVI swath data (right column of Figure 1) that queries the previous 20 days for up to six pieces of NDVI data to ensure a continuous grid populated at all pixels using the following formula at each grid point:

$$NDVI(j,i) = \begin{cases} \dfrac{\sum_{n=1}^{m} NDVI_n \left(\dfrac{1.0}{DaysLate_n + 1} \right)}{\left(\dfrac{1.0}{DaysLate_n + 1} \right)}; m \geq 1 \\ \text{where } m = \#\text{ of NDVIvalues at } (j,i) \\ -9.999 \text{ (missing)}; m = 0 \end{cases} \quad (2).$$

4.2 Calculating MODIS GVF for use in LIS

The GVF from the MODIS NDVI data is calculated on the identical 0.01-deg grid following the procedures outlined in Zeng et al. (2000) and Miller et al. (2006). The GVF at each grid point is computed as a function of the IGBP/MODIS vegetation class by first determining the maximum NDVI at each grid point using the previous *t* NDVI composites, where *t* is ideally a running collection of the previous 365 days of NDVI composites. However, since a full year of NDVI composites has not yet been collected, we used all the composites from June to October to determine the $NDVI_{max}$ values at each grid point. In the future, the $NDVI_{max}$ values will be determined based on the previous year of daily NDVI composites. Once the $NDVI_{max}$ is found at each grid point, the $NDVI_{max}$ values are sorted as a function of land use class. All grid points with the same land use class are lumped together into a single distribution of $NDVI_{max}$ values, which are then sorted to find the 90^{th} percentile $NDVI_{max}$ for each land use class, and the 5^{th} percentile for the barren land use class. The GVF can then be computed as a function of vegetation (land use) class using the following formula:

$$GVF_i = \frac{NDVI_i - NDVI_S}{NDVI_{V,i} - NDVI_S} \qquad (3),$$

where $NDVI_i$ is the actual NDVI composite value at a grid point *i*, $NDVI_S$ is a global constant that corresponds to the 5^{th} percentile of the array of $NDVI_{max}$ values of the barren vegetation class, and $NDVI_{V,i}$ is the 90^{th} percentile of $NDVI_{max}$ values for the vegetation class at grid point *i*.

Missing NDVI pixels are filled with the AVHRR monthly climatological GVF data, which should mainly impact winter composites when snow cover (or persistent cloud cover) prevents an adequate NDVI reading. Since evapotranspiration is much less substantial in the surface energy budget during the winter months, the impact of filling data with the AVHRR monthly climatology should be minimal.

The new daily GVF dataset then replaces the monthly climatological GVF database based on five years of AVHRR observations currently available to the Noah LSM in both LIS and the public version of the WRF model. The much higher spatial resolution (1 km versus 0.15 degree) and daily updates based on real-time satellite observations have the capability to greatly improve the simulation of the surface energy budget in the Noah LSM within LIS and WRF.

5. PRELIMINARY IMPACT RESULTS

To measure the sensitivities and impacts, the LIS is configured to use the Noah LSM as run at NCEP and within the WRF model. For the initial tests, the LIS-Noah is run in an uncoupled, or offline mode with atmospheric analyses from the North American Land Data Assimilation System (NLDAS, Mitchell et al. 2004) and the Global Data Assimilation System (GDAS, Derber et al. 1991) providing the required input fields to drive the LSM integrations. The NLDAS is used where possible, while outside of the NLDAS domain, the GDAS analyses are invoked. The GDAS forcing fields of downward-directed longwave radiation, surface pressure, 2-m air temperature, and 2-m specific humidity are corrected topographically via lapse-rate and hypsometric adjustments using the elevation data differences between the LIS and native GDAS forcing grids (Cosgrove et al. 2003).

A fine-scale model equilibrium state is not necessary for the current set of comparison simulations; therefore, a long-term spin-up run of LIS-Noah is not made at this time. Instead, the LIS is configured to run on a CONUS-scale 4-km grid identical to the real-time WRF grid run by the National Severe Storms Laboratory in support of Hazardous Weather Testbed and the Storm Prediction Center (Kain et al. 2010). The CONUS 4-km offline LIS runs are made from 1 June to 31 October 2010, spanning the warm season months. In addition, a 1-km LIS run is made during the month of June centered on Montana, helping to depict the green-up throughout the month as well as the importance of higher-resolution GVF in areas of complex terrain.

An example comparison of the June GVFs on the full-resolution 0.01° grid is given in Figure 2. Overall, the SPoRT MODIS GVFs tend to have higher greenness values across much of the High Plains, far southeastern U.S., Mexico, and the southwestern U.S. Areas that have lower GVFs in the SPoRT product include the Great Lakes and northeastern U.S., the Appalachians, and portions of the northern Rockies (Figure 2, bottom panel). Worth noting is the much greater amount of detail seen in the SPoRT GVF dataset, particularly in the inter-mountain West. The large-scale patterns are consistent, however, helping to affirm the soundness of the SPoRT GVFs.

Zooming into the Montana high-resolution run reveals detailed differences between the AVHRR climatology and the SPoRT MODIS GVFs related to the ability to resolve complex terrain features. The AVHRR climatology appears quite smooth on this scale showing a minimum in GVF over the prairies of eastern Montana, northern Wyoming, western South Dakota, and central Idaho (Figure 3, top). A broad maximum exists along the Montana-Idaho border associated with the high terrain along the Continental Divide. Meanwhile, the SPoRT GVFs show much greater detail able to resolve small river basins with locally higher GVF, and relatively lower GVFs in the higher ridgetops in northwestern Wyoming and along the Montana-Idaho border (Figure 3, middle and bottom). The SPoRT GVFs generally depict much higher GVFs along the High Plains in the western Dakotas and eastern Montana (Figure 3, bottom).

These variations in GVF directly impact the surface energy budget through the partitioning of sensible and latent heat fluxes. With the ability to better resolve the ridgetops, the LIS run with the SPoRT GVFs depict substantially lower latent heat fluxes up to 100 W m^{-2} over the high terrain where the GVFs are lower than the AVHRR climatology (Figure 4). Meanwhile, the latent heat fluxes are locally-regionally higher by about the same amount over parts of the High Plains where the SPoRT GVFs are higher (Figure 4, bottom). Worth noting in the difference field is the amount of local,

detailed variations that are consistent with the terrain elevation features of this region (not shown).

Finally, the higher GVFs over the High Plains of eastern Montana and the western Dakotas are consistent with fairly significant positive precipitation anomalies during May and June 2010. The top panel of Figure 5 shows that much of the High Plains experienced very substantial amounts of rainfall during May of 150% to as much as 600% of normal rainfall, especially northeastern Montana to western South Dakota. Meanwhile, western Montana and northern Idaho had generally normal to below normal rainfall during May where the SPoRT/MODIS GVFs are somewhat lower than the AVHRR climatology. The month of June 2010 saw much of the same, but with the entire region experiencing above-average precipitation (Figure 5, bottom). Precipitation is not necessarily the sole driver in producing anomalies in GVFs; however, on a regional scale there is certainly a strong qualitative correlation between the monthly precipitation anomalies and the deviations between the SPoRT/MODIS and AVHRR climatology GVFs.

Additional preliminary results from the 4-km NSSL CONUS domain runs during the 2010 warm season will be shown in the companion presentation.

6. SUMMARY AND FUTURE WORK

Future efforts will involve incorporating the experimental SPoRT GVF data set into coupled model runs in which the LIS framework is called from within the Advanced Research WRF (ARW, Skamarock et al. 2008) model. With LIS being tightly coupled to the ARW (Kumar et al. 2007), this framework enables a seamless incorporation of the experimental daily GVF data into the WRF model. Such experiments would demonstrate the impacts and utility of the high-resolution, daily updated vegetation data set by comparing the surface energy budget using the SPoRT GVF to that using the climatological means. In addition, validation of near-surface meteorological variables and quantitative precipitation will be conducted to quantify the level of improvement in the model forecasts. Also, the development of a global 1-km daily-updated MODIS GVF product would be beneficial to the operational weather community.

Finally, SPoRT also seeks to collaborate with its partners and current users of the coupled LIS/ARW framework. The Air Force Weather Agency (AFWA) runs the LIS/ARW coupled framework operationally for the numerous regional model forecast domains across the globe. In fact, AFWA has been simultaneously experimenting with a similar such GVF data set in their coupled LIS/ARW model (Ruhge and Barlage 2011, this conference). It is the intent of SPoRT to develop and transition a high-quality dataset that can be used by its partner organizations to improve the short-term forecast process.

7. ACKNOWLEDGEMENTS/DISCLAIMER

This research was funded by Dr. Tsengdar Lee of the NASA Science Mission Directorate's Earth Science Division in support of the SPoRT program at the NASA MSFC. Computational resources for this work were provided by the NASA Center for Computational Sciences at the NASA Goddard Space Flight Center. Mention of a copyrighted, trademarked or proprietary product, service, or document does not constitute endorsement thereof by the authors, ENSCO Inc., SAIC, USRA, the SPoRT Center, the National Aeronautics and Space Administration, or the United States Government. Any such mention is solely for the purpose of fully informing the reader of the resources used to conduct the work reported herein.

8. REFERENCES

Barlage, M., X. Zeng, H. Wei, and K. E. Mitchell, 2005: A global 0.05° maximum albedo dataset of snow-covered land based on MODIS observations. *Geophys. Res. Lett.,* **32,** L17405, doi:10.1029/2005GL022881.

Briegleb, B. P., P. Minnis, V. Ramanathan, and E. Harrison, 1986: Comparison of regional clear-sky albedos inferred from satellite observations and model computations. *J. Climate Appl. Meteor.,* **25,** 214-226.

Case, J. L., W. L. Crosson, S. V. Kumar, W. M. Lapenta, and C. D. Peters-Lidard, 2008: Impacts of High-Resolution Land Surface Initialization on Regional Sensible Weather Forecasts from the WRF Model. *J. Hydrometeor.,* **9,** 1249-1266.

Case, J. L., S. V. Kumar, J. Srikishen, and G. J. Jedlovec, 2011: Improving numerical weather predictions of summertime precipitation over the southeastern U.S. through a high-resolution initialization of the surface state. *Wea. Forecasting, In Review.*

Chen, F., and J. Dudhia, 2001: Coupling an advanced land-surface/hydrology model with the Penn State/NCAR MM5 modeling system. Part I: Model description and implementation. *Mon. Wea. Rev.,* **129,** 569-585.

Cosgrove, B. A., and Coauthors, 2003: Real-time and retrospective forcing in the North American Land Data Assimilation System (NLDAS) project. *J. Geophys. Res.,* **108(D22),** 8842, doi:10.1029/2002JD003118, 2003.

Crawford, T. M., D. J. Stensrud, F. Mora, J. W. Merchant, and P. J. Wetzel, 2001: Value of incorporating satellite-derived land cover data in MM5/PLACE for simulating surface temperatures. *J. Hydrometeor.,* **2,** 453-468.

Darden, C. B., D. J. Nadler, B. C. Carcione, R. J. Blakeslee, G. T. Stano, and D. E. Buechler, 2010: Utilizing total lightning information to diagnose convective trends. *Bull. Amer. Meteor. Soc.,* **91,** 167-175.

Derber, J. C., D. F. Parrish, and S. J. Lord, 1991: The new global operational analysis system at the National Meteorological Center. *Wea. Forecasting,* **6,** 538-547.

Ek, M. B., K. E. Mitchell, Y. Lin, E. Rogers, P. Grunmann, V. Koren, G. Gayno, and J. D. Tarpley, 2003: Implementation of Noah land surface model advances in the National Centers for Environmental Prediction operational mesoscale Eta model. *J. Geophys. Res.,* **108 (D22),** 8851, doi:10.1029/2002JD003296.

Friedl, M. A., D. Sulla-Menashe, B. Tan, A. Schneider, N. Ramankutty, A. Sibley, and X. Huang, 2010: MODIS Collection 5 global land cover: Algorithm refinements and characterization of new datasets. *Remote Sens. Environ.,* **114,** 168-182.

Goodman, S. J., W. M. Lapenta, G. J. Jedlovec, J. C. Dodge, and J. T. Bradshaw, 2004: The NASA Short-term Prediction Research and Transition (SPoRT) Center: A collaborative model for accelerating research into operations. Preprints, *20th Conf. on Interactive Information Processing Systems (IIPS) for Meteorology, Oceanography, and Hydrology,* Seattle, WA, Amer. Meteor. Soc., P1.34. [Available online at http://ams.confex.com/ams/pdfpapers/70210.pdf]

Gutman, G. and A. Ignatov, 1998: Derivation of green vegetation fraction from NOAA/AVHRR for use in numerical weather prediction models. *Int. J. Remote Sensing,* **19,** 1533-1543.

Haines, S. L., G. J. Jedlovec, and S. M. Lazarus, 2007: A MODIS sea surface temperature composite for regional applications. *IEEE Trans. Geosci. Remote Sens.,* **45,** 2919-2927.

James, K. A., D. J. Stensrud, and N. Yussouf, 2009: Value of real-time vegetation fraction to forecasts of severe convection in high-resolution models. *Wea. Forecasting,* **24,** 187-210.

Janjic, Z. I., 2003: A Nonhydrostatic Model Based on a New Approach. *Meteorology and Atmospheric Physics,* **82,** 271-285.

Janjic, Z. I., J. P. Gerrity, Jr. and S. Nickovic, 2001: An Alternative Approach to Nonhydrostatic Modeling. *Mon. Wea. Rev.,* **129,** 1164-1178.

Jiang, L., and Coauthors, 2010: Real-time weekly global green vegetation fraction derived from advanced very high resolution radiometer-based NOAA operational global vegetation index (GVI) system. *J. Geophys. Res.,* **115,** D11114, doi:10.1029/2009JD013204.

Kain, J. S., S. R. Dembek, S. J. Weiss, J. L. Case, J. J. Levitt, and R. A. Sobash, 2010: Extracting unique information from high-resolution forecast models: Monitoring selected fields and phenomena every time step. *Wea. Forecasting,* **25,** 1536-1542.

Kumar, S. V., and Coauthors, 2006. Land Information System – An Interoperable Framework for High Resolution Land Surface Modeling. *Environmental Modeling & Software,* **21 (10),** 1402-1415, doi:10.1016/j.envsoft.2005.07.004.

Kumar, S. V., C. D. Peters-Lidard, J. L. Eastman, and W.-K. Tao, 2007: An integrated high-resolution hydrometeorological modeling testbed using LIS and WRF. *Environmental Modeling & Software,* **23 (2),** 169-181, doi: 10.1016/j.envsoft.2007.05.012.

Kurkowski, N. P., D. J. Stensrud, and M. E. Baldwin, 2003: Assessment of implementing satellite-derived land cover data in the Eta model. *Wea. Forecasting,* **18,** 404-416.

Loveland, T. R., B. C. Reed, J. F. Brown, D. O. Ohlen, Z. Zhu, L. Yang, and J. W. Merchant, 2000: Development of a global land cover characteristics database and IGBP DISCover from 1 km ABHRR data. *Int. J. Remote Sensing,* **21,** 1303-1330.

Miller, D. A. and R. A. White, 1998: A Conterminous United States multi-layer soil characteristics data set for regional climate and hydrology modeling. *Earth Interactions*, 2. [Available on-line at http://EarthInteractions.org].

Miller, J. M. Barlage, X. Zeng, H. Wei, K. Mitchell, and D. Tarpley, 2006: Sensitivity of the NCEP/Noah land surface model to the MODIS green vegetation fraction data set. *Geophys. Res. Lett.,* **33,** L13404, doi:10.1029/2006GL026636.

Mitchell, K. E., and Coauthors, 2004: The multi-institution North American Land Data Assimilation System (NLDAS): Utilization of multiple GCIP products and partners in a continental distributed hydrological modeling system. *J. Geophys. Res.,* **109,** D07S90, doi:10.1029/2003JD003823.

Ruhge, R. L., and M. Barlage, 2011: Integrating a real-time green vegetation fraction (GVF) product into the Land Information System (LIS). Preprints, *15th Symp. on Integrated Observing and Assimilation Systems for the Atmosphere, Oceans, and Land Surface,* J14.4.

Skamarock, W. C., J. B. Klemp, J. Dudhia, D. O. Gill, D. M. Barker, M. G. Duda, X-Y. Huang, W. Wang and J. G. Powers, 2008: A Description of the Advanced Research WRF Version 3, NCAR Technical Note, NCAR/TN–475+STR, 123 pp. [Available on-line at: http://www.mmm.ucar.edu/wrf/users/docs/arw_v3.pdf]

Stano, G. T., K. K. Fuell, and G. J. Jedlovec, 2010: NASA SPoRT GOES-R Proving Ground activities. Preprints, *6th Annual Symposium on Future National Operational Environmental Satellite Systems-NPOESS and GOES-R,* Atlanta, GA, Amer. Meteor. Soc., 8.2. [Available online at http://ams.confex.com/ams/pdfpapers/163879.pdf]

Zeng, X., R. E. Dickinson, A. Walker, M. Shaikh, R. S. DeFries, and J. Qi, 2000: Derivation and evaluation of global 1-km fractional vegetation cover data for land modeling. *J. Appl. Meteor.,* **39,** 826-839.

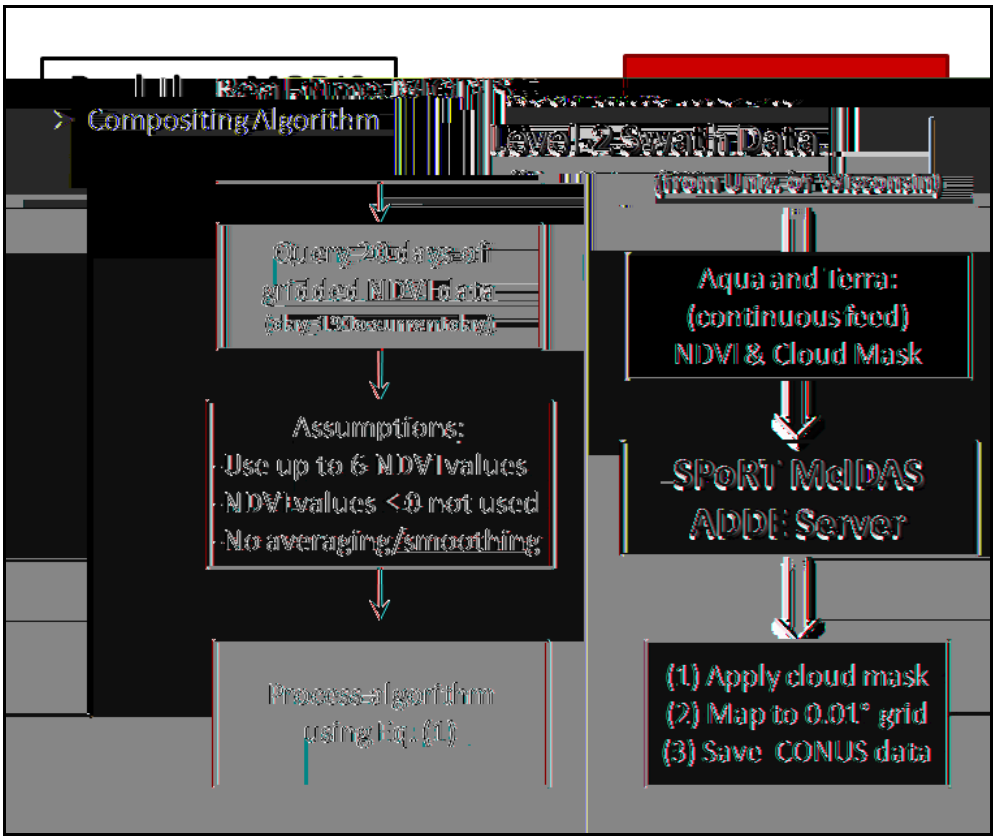

Figure 1. Diagram of the data and process flow of the SPoRT NDVI compositing algorithm.

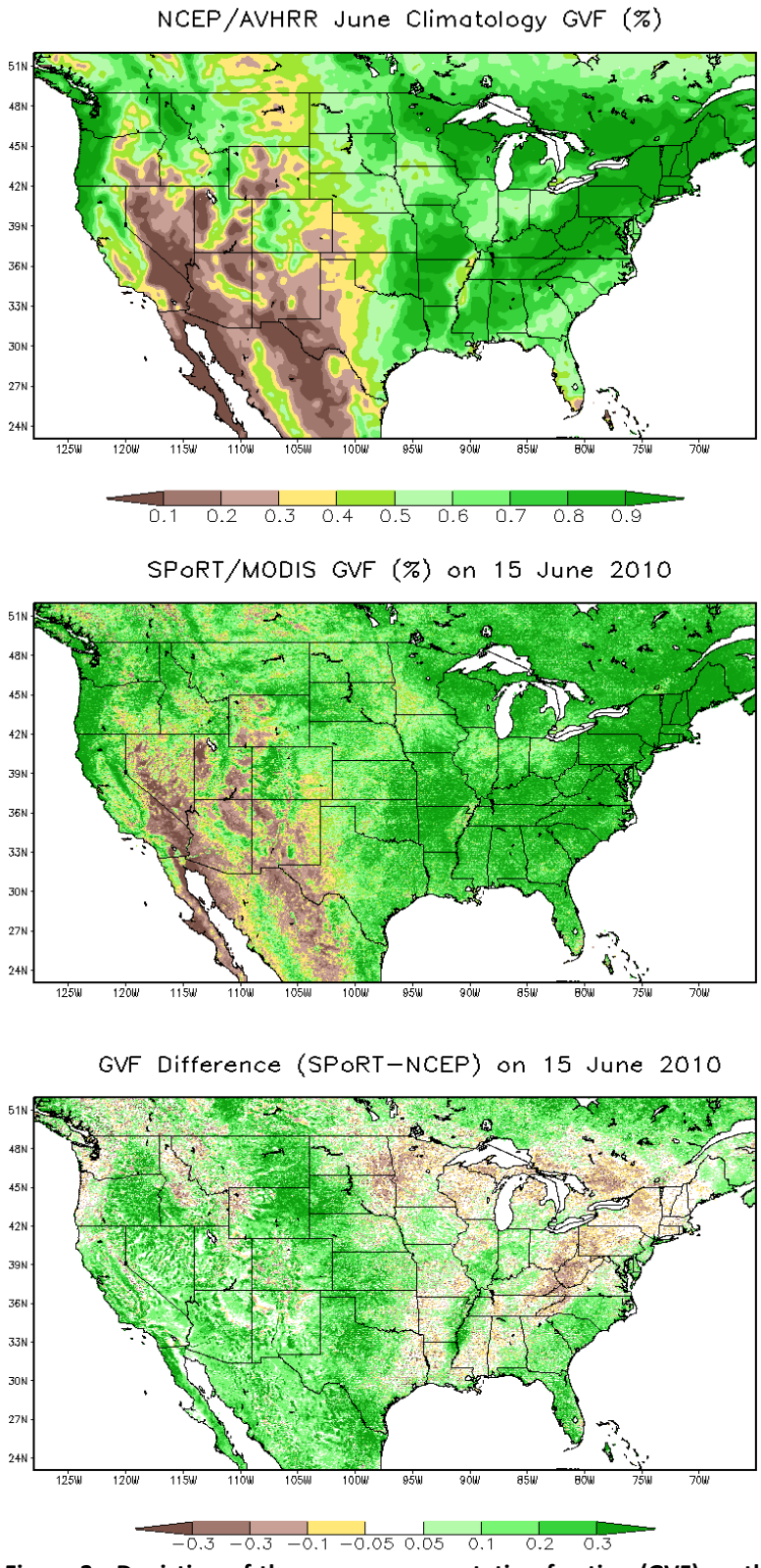

Figure 2. Depiction of the greenness vegetation fraction (GVF) on the SPoRT CONUS 0.01° domain from 15 June for the current NCEP/AVHRR climatology (top), the SPoRT daily GVF (middle), and the difference (SPoRT – NCEP, bottom).

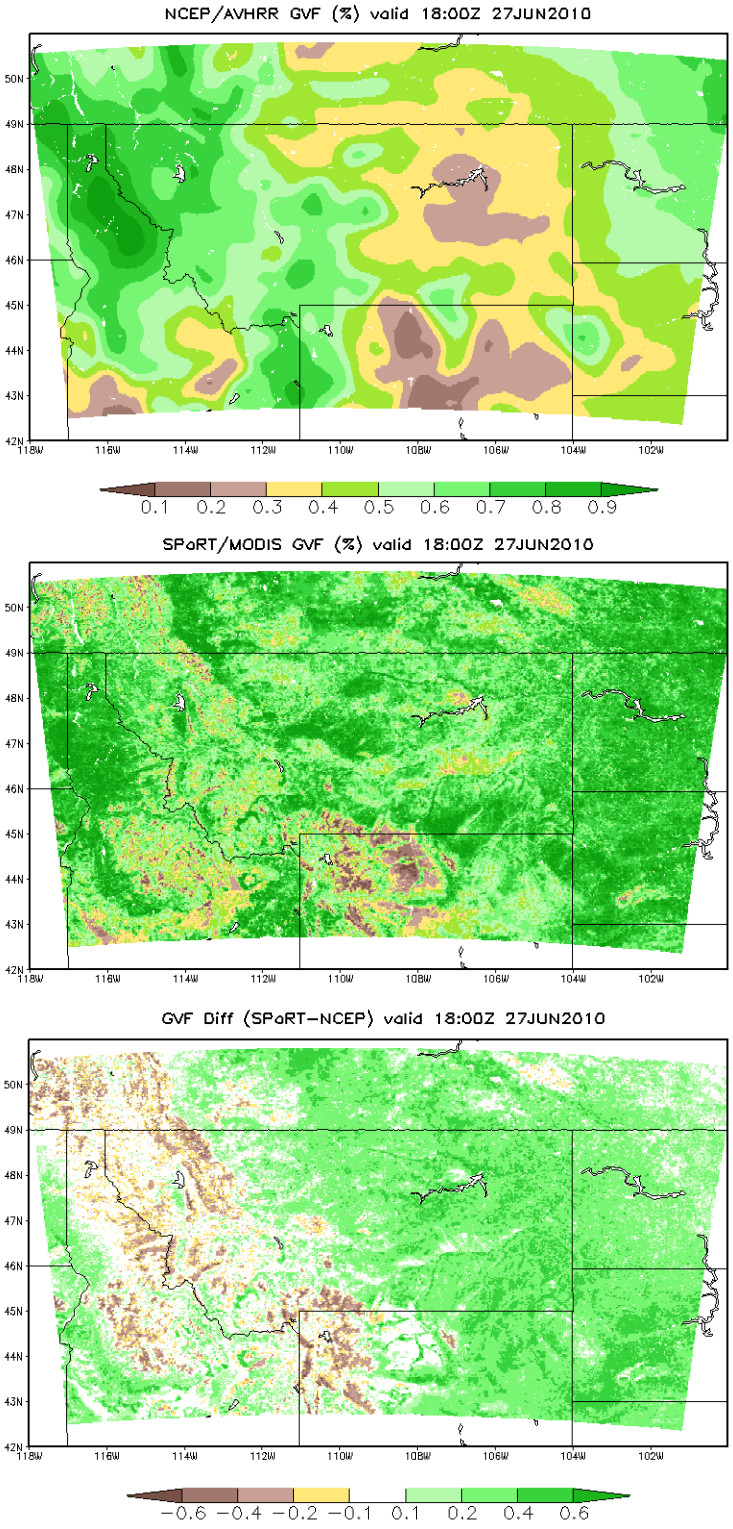

Figure 3. Depiction of the greenness vegetation fraction (GVF) on a 0.01° resolution grid centered on Montana at 1800 UTC 27 June for the interpolated NCEP/AVHRR climatology (top), the SPoRT daily GVF (middle), and the difference (SPoRT – NCEP, bottom).

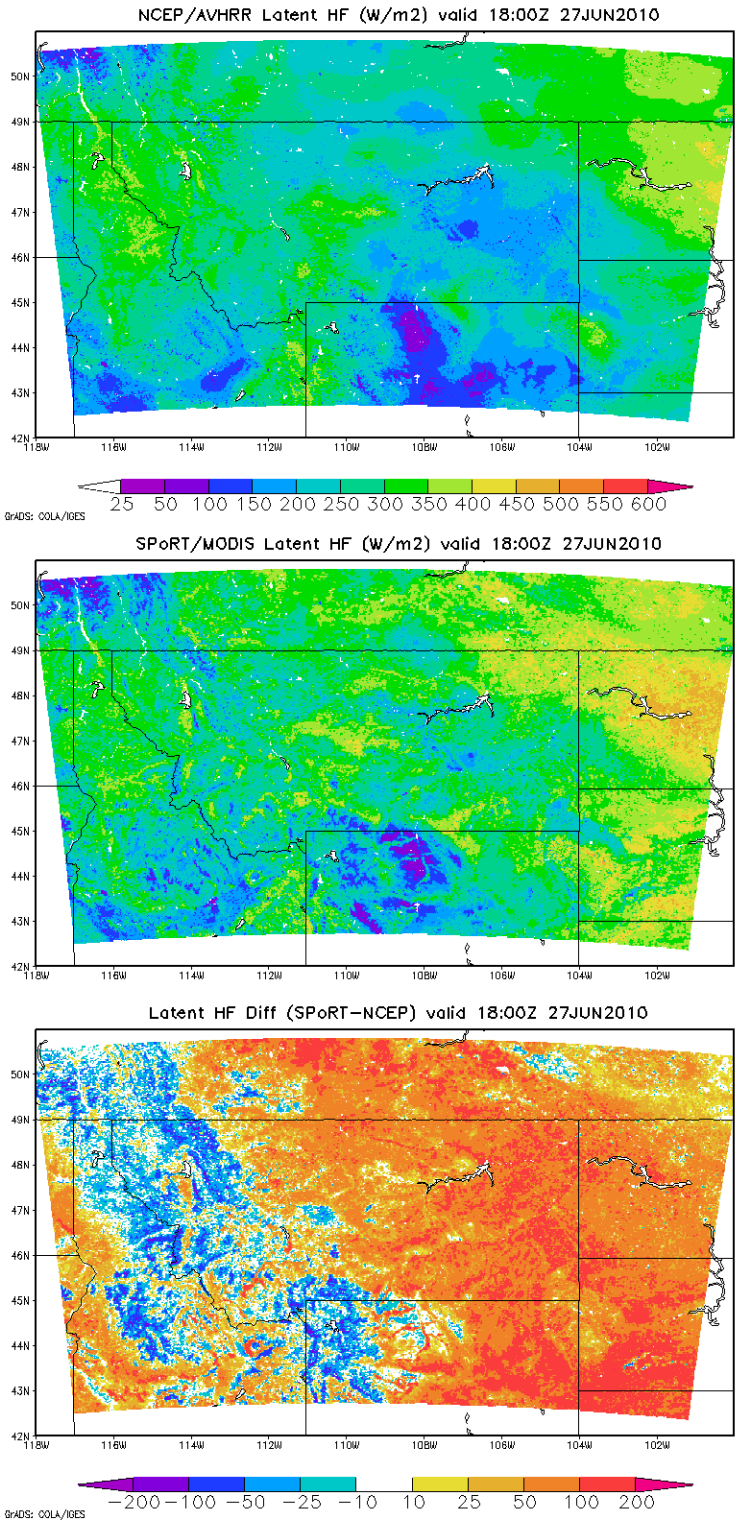

Figure 4. Depiction of the LIS-Noah latent heat flux (W m^{-2}) on a 0.01° resolution grid centered on Montana at 1800 UTC 27 June for the interpolated NCEP/AVHRR climatology (top left), the SPoRT daily GVF (top right), and the difference (SPoRT – NCEP, bottom panel).

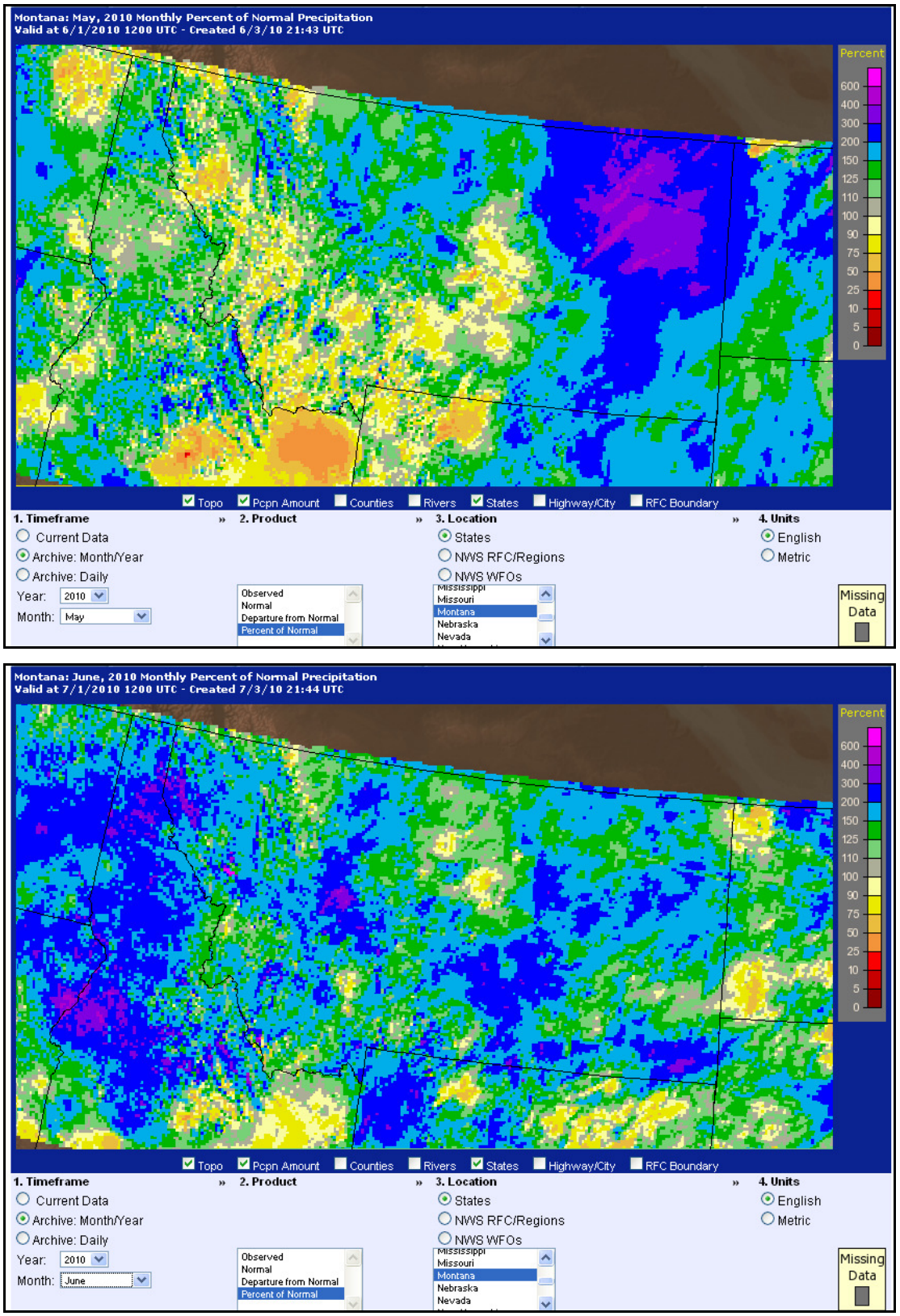

Figure 5. Monthly percent of normal precipitation for May 2010 (top), and June 2010 (bottom), produced by the Advanced Hydrological Prediction Service and available at http://water.weather.gov/precip/.